

## An ellipsoidal model for studying response of head impacts

MAHDI HEYDARI<sup>1</sup>, SAEID JANI<sup>2\*</sup>

<sup>1</sup>Department of Mechanical Engineering, Sharif University of Technology, Azadi Avenue, Tehran, Iran.

<sup>2</sup>Department of Mechanical Engineering, Office of Golpayegan University of Technology, Azadi Avenue, Tehran, Iran.

The objective of this study was to propose a new analytical model for studying response of head impacts. Head is modeled by fluid-filled ellipsoidal shell of inconstant thickness impacted by a solid elastic sphere. Modeling the head as an ellipsoid is more realistic than modeling it as a sphere, the previous model existing in the literature [3]–[8]. In this model, the effect of Hertzian contact stiffness and local shell stiffness are combined to derive explicit equations for impact duration, the peak force transmitted to head, and the head injury criterion. One of the advantages of the model presented is sensitivity to the site of impact. A comparison between the present analytical results with the analytical data from spherical model [8] has been done to verify the validation of the present model.

*Key words: ellipsoidal model, head impact, shell stiffness, Hertzian contact stiffness*

### 1. Introduction

Annual head injury statistics represent an enormous emotional and financial burden of 1.5 million people sustaining a Traumatic Brain Injury (TBI), 230,000 hospitalizations, 50,000 deaths, and 80,000–90,000 people experiencing the onset of long-term disability, and an estimated \$56 billion in annual costs for TBI in the USA [1], [2]. Such a big problem caused researchers to take many attempts at modeling head impacts based on analytical, numerical, experimental, or cadaveric methods.

ANZELIUS developed an early analytical model for head impact that assumed the head to be a rigid spherical shell filled with inviscid compressible fluid [3]. His formulation involved an axisymmetric solution of the wave equation in spherical coordinates. GUTTINGER used an identical model and formulation, but in his analysis the fluid-filled spherical vessel was initially at rest and instantaneously acceler-

ated to a constant velocity instead of translating the shell with a constant velocity and bringing it to a sudden stop [4]. They concluded that the initial velocity input produced a compression wave at the point of impact. The obvious defects of the fluid-filled rigid shell model, such as producing cavitation phenomena in the center and causing an infinite speed of wave propagation, led GOLDSMITH to a suggestion of an analytical or numerical solution of a fluid-filled elastic shell [5]. ENGIN proposed a model based on linear shell theory which includes both membrane and bending effects, and investigated determination of the dynamic response of a fluid-filled spherical shell subjected to a local radial impulsive load – a normal delta function [6]. The normal delta-function loading was extended to loadings of finite duration by KENNER and GOLDSMITH [7]. YOUNG proposed a model to predict the impacting with a solid elastic sphere by combining the Hertzian contact stiffness, the effective local membrane, and the bending stiffness [8].

---

\* Corresponding author: Saeid Jani, Department of Mechanical Engineering, Office of Golpayegan University of Technology, Azadi Avenue, Tehran, Iran. E-mail: jani@gut.ac.ir

Received: September 11th, 2009

Accepted for publication: February 28th, 2010

Because of the complexity of head, developing an accurate analytical model is nearly impossible. So, many numerical models were provided to cover the complexity of head and discuss the influence of the various parameters on model results that could be found in open literature reviews by KHALIL and VIANO [9], SAUREN and CLAESSENS [10], VOO et al. [11], and RAUL et al. [12].

In all the pervious analytical models mentioned above, a constant thickness spherical model for head geometry has been used. In this paper, a more realistic model for head has been developed by assuming the head as an inconstant thickness ellipsoid. The equations of peak force transmitted, impact duration, and Head Injury Criterion (HIC) have been derived and their results have been shown for any given point of head. For verification of the model proposed analytical results are compared with the existing data [8].

## 2. Theoretical model

Based on the geometry of the head, in the present study the head has been modeled as an ellipsoidal shell which is more realistic compared with the spherical model. Menton to top of head, glabella to back of head (head length), and head breadth could be used as the three axes of the ellipsoid with regard to the head geometry. The shell is filled with fluid that is assumed to be water. The mechanical properties of water are very similar to the brain and the cerebrospinal fluid properties (density 1040 kg/m<sup>3</sup>, bulk modulus 2.19 GPa for brain, and density 1004 kg/m<sup>3</sup>, bulk modulus 2.19 GPa for cerebro-spinal fluid [13] compared to density 1000 kg/m<sup>3</sup>, and bulk modulus 2.2 GPa for water), and therefore, one can find in literature that water has frequently been used for modeling them.

Physically, the model, as shown in figure 1, represents an impact of a solid sphere of mass  $m_{sol}$  traveling at a velocity  $v_{sol}$  with a fluid-filled ellipsoidal shell of mass  $m_s$  traveling at a velocity  $v_s$ .

The shell has the radii  $a$ ,  $b$ , and  $c$  ( $a > b > c$ ), the inconstant thickness  $h$  – as a function of coordinates of head points and it is assumed that its material properties are homogeneous and isotropic with Young's modulus  $E_{sh}$ , Poisson's ratio  $\nu_{sh}$  and density  $\rho_{sh}$ . The solid sphere has the radius  $R_{sol}$  and the homogeneous and isotropic material properties with Young's modulus  $E_{sol}$ , Poisson's ratio  $\nu_{sol}$  and density  $\rho_{sol}$ .

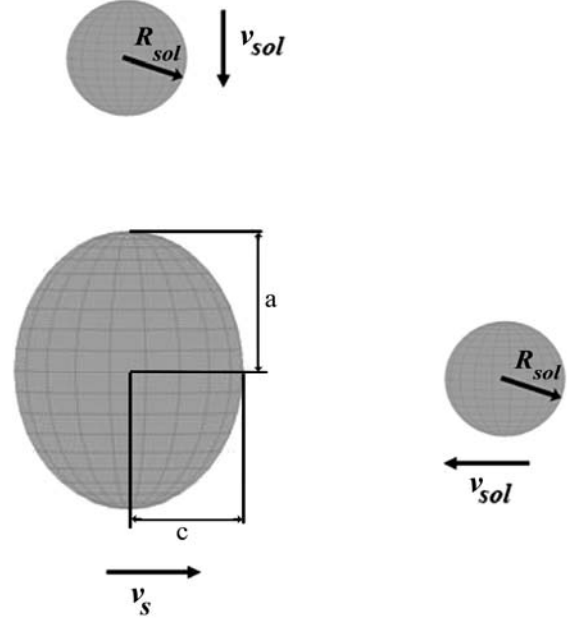


Fig. 1. Illustrative representation of the ellipsoidal model

### 2.1. Laws of contact

The contact stiffness is considered to be the sum of the Hertzian contact stiffness and the thin shell contact stiffness.

#### 2.1.1. The Hertz law of contact

Using the Hertz law of contact, the force-deformation law is [14]

$$F = k_H \Delta x_H^{3/2}, \quad (1)$$

where  $F$  is the applied force,  $\Delta x_H$  is the approach and represents the maximum relative compression of the two bodies, and the Hertzian contact stiffness  $k_H$  is given by:

$$k_H = \frac{4}{3} R^{*1/2} E^*, \quad (2)$$

where:

$$\frac{1}{E^*} = \frac{(1-\nu_{sol}^2)}{E_{sol}} + \frac{(1-\nu_{sh}^2)}{E_{sh}} \quad (3)$$

and [15]:

$$\frac{1}{R^*} = \frac{1}{R_{sol}} + \frac{1}{2R_{1sh}} + \frac{1}{2R_{2sh}}, \quad (4)$$

where  $R_{1sh}$  and  $R_{2sh}$  are two principal radii of curvature at the point of impact.

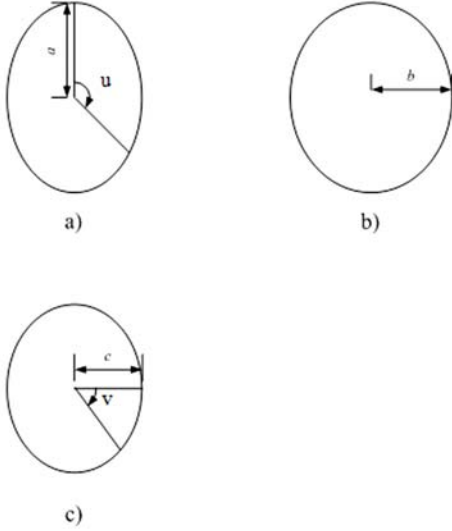


Fig. 2. Geometry of the ellipsoidal model and the coordinates system; a) front view, b) side view, c) top view of head model

By using the spherical coordinates system shown in figure 2, the Gaussian and mean curvatures, represented by  $K$  and  $H$ , respectively, are given by [16]:

$$K(u, v) = \frac{a^2 b^2 c^2}{[a^2 b^2 \cos^2 v + c^2 (b^2 \cos^2 u + a^2 \sin^2 u) \sin^2 v]^2}, \quad (5)$$

$$H(u, v) = \frac{abc[3(a^2 + b^2) + 2c^2 + (a^2 + b^2 - 2c^2)\cos(2v) - 2(a^2 - b^2)\cos(2u)\sin^2 v]}{8[a^2 b^2 \cos^2 v + c^2 (b^2 \cos^2 u + a^2 \sin^2 u) \sin^2 v]^{3/2}}, \quad (6)$$

where  $u$  and  $v$  are the azimuth and the zenith angles in the spherical coordinates system ( $u \in [0, 2\pi)$ ,  $v \in [0, \pi]$ ).

The principal radii of curvature  $R_{1sh}$  and  $R_{2sh}$  are given by [16]:

$$R_{1sh}(u, v) = (H + \sqrt{H^2 - K})^{-1}, \quad (7)$$

$$R_{2sh}(u, v) = (H - \sqrt{H^2 - K})^{-1}. \quad (8)$$

### 2.1.2. Thin shell stiffness

The force-deformation law for the thin empty shells is:

$$F = k_{sh} \Delta x_{sh}, \quad (9)$$

where  $k_{sh}$  – the shell stiffness – is given by [17]

$$K_{sh}(u, v) = \frac{2.3 E_{sh} h^2(u, v)}{R_{sh}(u, v) (1 - v_{sh}^2)^{1/2}}. \quad (10)$$

Since the mean curvature  $H$  locally describes the curvature of surface, it could be used for the curvature of shell at the point of impact. So, the radius of shell  $R_{sh}$  at the point of impact can be calculated as:

$$R_{sh}(u, v) = \frac{1}{H(u, v)}. \quad (11)$$

It was shown by YOUNG and MORFEY [18] that the bulk modulus of fluid has no effect on the stiffness of shells, and therefore equations (9) and (10) are appropriate to use for both (compressible or incompressible) fluid-filled and empty shells. Also as seen in equations (1)–(4), the fluid has no effect on the Hertzian contact stiffness. Thus, the analytical model proposed in this study is applicable to both fluid-filled and empty shells.

## 2.2. Explicit equations

With the same procedure as in YOUNG [8], the equations of impact duration  $T_p$  and peak force transmitted  $F_p$  can be obtained as:

$$T_p = \pi \sqrt{\frac{3}{4} \left(\frac{16}{15}\right)^{1/5} \frac{m^{*4/5}}{R^{*2/5} E^{*4/5} \Delta v^{2/5}} + \frac{m^* R_{sh} \sqrt{(1 - v_{sh}^2)}}{2.3 E_{sh} h^2}}, \quad (12)$$

$$F_p =$$

$$\frac{R^{*1/5} E^{*2/5} m^{*3/5} \Delta v^{6/5} E_{sh}^{1/12} h}{\left[ \frac{1}{2.3} R^{*2/5} E^{*4/5} m^{*1/5} \Delta v^{2/5} R_{sh} \sqrt{(1 - v_{sh}^2)} + \frac{3}{4} \left(\frac{16}{15}\right)^{1/5} E_{sh} h^2 \right]^{1/2}}, \quad (13)$$

where

$$\Delta v = v_s - v_{sol} \quad \text{and} \quad \frac{1}{m^*} = \frac{1}{m_s} + \frac{1}{m_{sol}}. \quad (14)$$

These equations are the same as equations reported by YOUNG [8] for the spherical model except that in the ellipsoidal model,  $R_{sh}$  and  $R^*$  are obtained from equations (4), (7), (8) and (11), but in YOUNG [8],  $R_{sh}$  is the radius of sphere that models the head and  $R^*$  is obtained from:

$$\frac{1}{R^*} = \frac{1}{R_{\text{sol}}} + \frac{1}{R_{\text{sh}}}. \quad (15)$$

The head injury criterion (HIC) was defined by the National Highway Traffic Society Administration (NHTSA) in 1972 as:

$$\text{HIC} = \left\{ (t_2 - t_1) \left( \frac{1}{(t_2 - t_1)} \int_{t_1}^{t_2} a(t) dt \right)^{5/2} \right\}_{\text{max}}, \quad (16)$$

in which  $t_1$  and  $t_2$  are the initial and final times of the interval during which HIC attains a maximum value and  $a(t)$  is the resultant translational head acceleration assumed to be:

$$a(t) = \frac{F_p}{m_s} \sin\left(\pi \frac{t}{T_p}\right). \quad (17)$$

For  $0 < t < T_p$ , by solving simultaneously:

$$\frac{\partial(\text{HIC})}{\partial t_1} = 0 \quad \text{and} \quad \frac{\partial(\text{HIC})}{\partial t_2} = 0, \quad (18)$$

equation (16) is simplified to [8]:

$$\text{HIC} = \frac{7.25311 F_p}{\pi^{5/2} m_s} T_p, \quad (19)$$

in which

$$T_p = \pi \sqrt{\frac{m^*}{k'_{\text{effec}}}}, \quad (20)$$

$$F_p = \Delta v \sqrt{m^* k'_{\text{effec}}}, \quad (21)$$

where  $k'_{\text{effec}}$  is comprised of the linearized Hertzian stiffness and the shell stiffness as an approximate linear stiffness of the system and is given by [8]:

$$k'_{\text{effec}} = \frac{R^{*2/5} E^{*4/5} m^{*1/5} \Delta v^{2/5} E_{\text{sh}} h^2}{\left[ \frac{1}{2.3} R^{*2/5} E^{*4/5} m^{*1/5} \Delta v^{2/5} R_{\text{sh}} \sqrt{(1 - v_{\text{sh}}^2)} + \frac{3}{4} \left( \frac{16}{15} \right)^{1/5} E_{\text{sh}} h^2 \right]} \quad (22)$$

So, the HIC defined by equation (19) is simplified to:

$$\text{HIC} = \frac{7.25311 m^* \Delta v}{\pi^{3/2} m_s}. \quad (23)$$

As seen, HIC depends only on  $\Delta v$ ,  $m_{\text{sol}}$  and  $m_s$ , and not on the radius of head nor impactor parameter. Thus, the ellipsoidal model yields identical result with that of the spherical model for the HIC.

### 3. Results and discussion

For simplification the thickness of the shell has been chosen constant and equal to average skull thickness  $h = 7.38$  mm [19], but as previously mentioned, it could be chosen inconstant. The other values of skull based on the 50<sup>th</sup> percentile (male) data for the glabella to the back of the head, the head length, and the head breadth [20], respectively, and the skull's bone data [6] are assumed to be:  $2a = 232$  mm,  $2b = 197$  mm,  $2c = 152$  mm,  $v_{\text{sh}} = 0.25$ ,  $\rho_{\text{sh}} = 2140$  kg/m<sup>3</sup>,  $E_{\text{sh}} = 13.79 \times 10^9$  N/m<sup>2</sup>,  $v_{\text{sol}} = 0.25$ ,  $\rho_{\text{sol}} = 7850$  kg/m<sup>3</sup>, and  $E_{\text{sol}} = 207 \times 10^9$  N/m<sup>2</sup>.

Thus, with these parameters for the head model,  $m_s$  becomes equal to 4.541 kg.

#### 3.1. Parametric study with varying impact site

The impactor velocity and mass were kept constant at 2.0 m/s and 0.25 kg, respectively, and then based on the analytical results, the effects of impact site on the peak force transmitted and the impact duration were explored.

As mentioned in section 2.2, HIC does not depend on the radius of head. Thus, the values of HIC for the ellipsoidal and spherical models are identical and its values are constant with the variation of impact site. The peak force transmitted and the impact duration for the ellipsoidal model are compared with those of the spherical model in figures 3 and 4a, b.

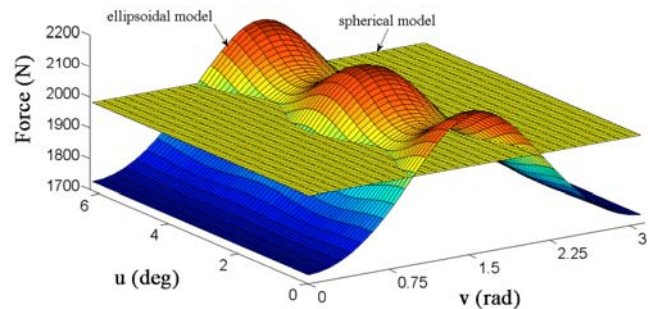


Fig. 3. Peak force results for different sites of impact using spherical [8] and ellipsoidal models ( $m_{\text{sol}} = 0.25$  kg,  $\Delta v = 2$  m/s)

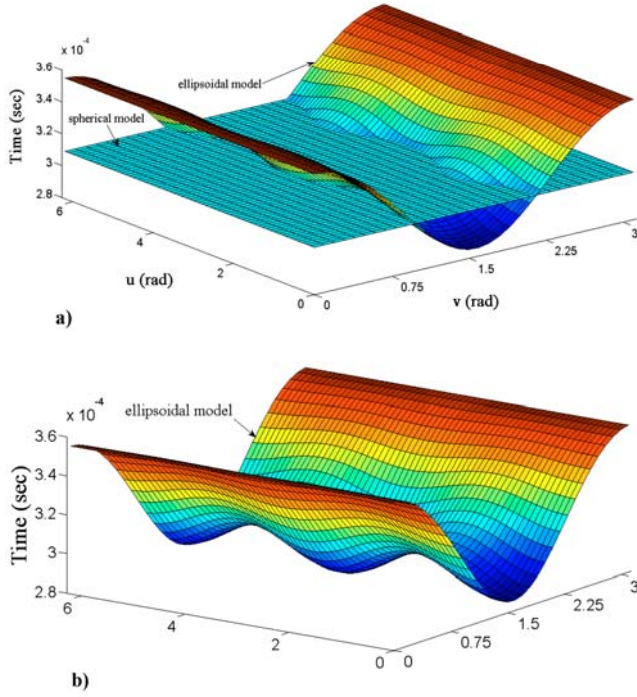


Fig. 4. Impact duration results for different sites of impact using spherical (a) [8] and ellipsoidal (a), (b) models ( $m_{sol} = 0.25$  kg,  $\Delta v = 2$  m/s)

In the ellipsoidal model, the peak force transmitted and the impact duration were changed with the impact site, whereas in the spherical model these parameters were constant. Also the variation of the azimuth angle ( $u$ ) has lower effect on the aforementioned parameters than the zenith angle ( $v$ ).

The maximum of peak force transmitted and the minimum of impact duration are observed at the position of  $v = \frac{\pi}{2}$ ,  $u = 0, \pi$ , i.e. at the points of semi-axis  $a$  (the major axis of ellipsoid). The minimum of peak force transmitted and the maximum of impact duration are observed at the position of  $v = 0, \pi$ , i.e. at the points of semi-axis  $c$  (the minor axis of ellipsoid). In comparison with the spherical model, the peak force transmitted at the points of semi-axes  $a$ ,  $b$ , and  $c$  is by 8.56%, 2.47% higher, and 12.9% lower, respectively. And the impact duration at the points of semi-axes  $a$ ,  $b$ , and  $c$  is by 7.85%, 2.39% lower, and 14.63%, respectively.

### 3.2. Parametric study with varying impactor mass

The impact velocity was kept constant at 2.0 m/s and the effect of impactor mass variation has been investigated.

Based on the two models, spherical and ellipsoidal, figures 5 and 6 show a comparison between the effect of impact at the points of semi-axes  $a$ , i.e.  $u = 0, \pi$ ,  $v = \frac{\pi}{2}$  (top of head),  $b$ , i.e.  $u = \frac{\pi}{2}, \frac{3\pi}{2}$ ,  $v = \frac{\pi}{2}$  (glabella and occiput), and  $c$ , i.e.  $v = 0, \pi$  (left- and right-hand sides of head). As seen in these figures, for impact at the points of semi-axes  $a$  and  $b$ , the ellipsoidal model has higher peak force transmitted and lower impact duration compared with the spherical model. And at the points of semi-axis  $c$ , the model presented has lower peak force transmitted and higher impact duration compared with the spherical model.

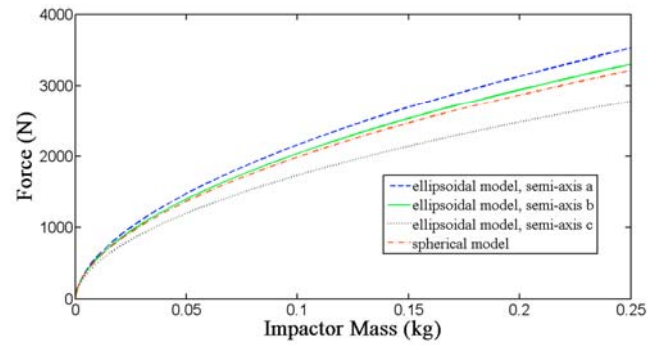


Fig. 5. Peak force results versus impactor mass using spherical [8] and ellipsoidal models for impact at the points of semi-axes  $a$ ,  $b$ , and  $c$  (constant impactor velocity of 2.0 m/s)

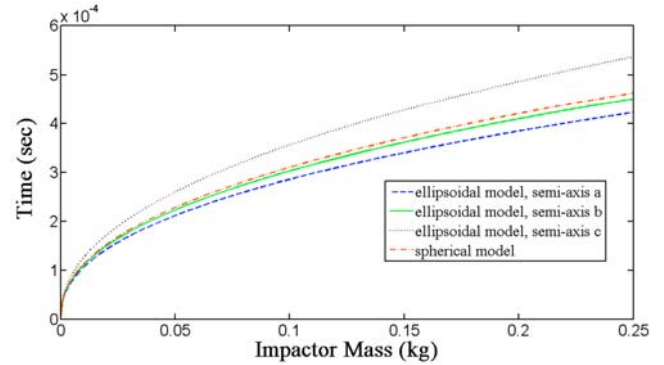


Fig. 6. Impact duration results versus impactor mass using spherical [8] and ellipsoidal models for impact at the points of semi-axes  $a$ ,  $b$ , and  $c$  (constant impactor velocity of 2.0 m/s)

### 3.3. Parametric study with varying impactor velocity

The maximum force transmitted, and the impact duration values against the impact velocity for impact at the points of semi-axes  $a$ ,  $b$ , and  $c$  for both the ellipsoidal and spherical models are shown in figures 7

and 8, respectively. The impactor mass was kept constant at 262 g.

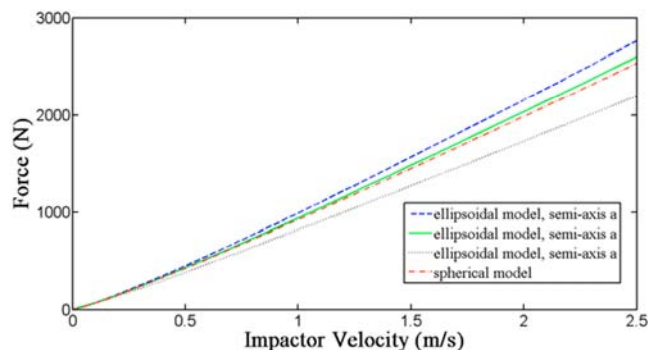


Fig. 7. Peak force results versus impactor velocity using spherical [8] and ellipsoidal models for impact at the points of semi-axes  $a$ ,  $b$ , and  $c$  (constant impactor mass of 262 g)

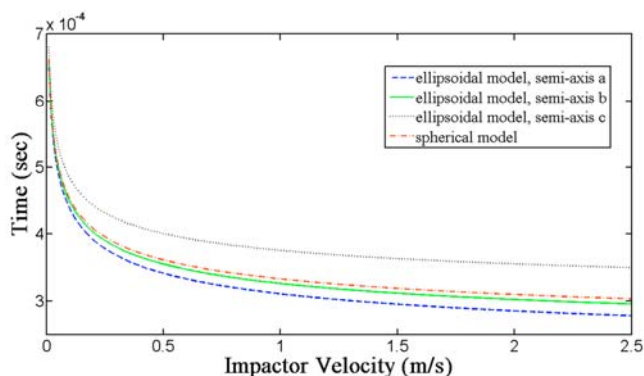


Fig. 8. Impact duration results versus impactor velocity using spherical [8] and ellipsoidal models for impact at the points of semi-axes  $a$ ,  $b$ , and  $c$  (constant impactor mass of 262 g)

For impact at the points of semi-axes  $a$  and  $b$ , the model proposed has higher peak force transmitted and lower impact duration compared with the spherical model. While, at the points of semi-axis  $c$ , the peak force transmitted is lower and the impact duration is higher than in the spherical model.

## 4. Conclusions

The ellipsoidal model was used to predict analytically the peak force transmitted, the impact duration, and the HIC. Head has been impacted by a spherical solid at any point of head and the results have been compared with those of the spherical model of head impact [8]. Sensitivity to the site of impact has been included in the present model. Based on the parametric study, it is shown that the peak force transmitted

and the impact duration are more sensitive to the zenith angle variation than to the azimuth angle.

Because the defined analytical HIC does not depend on the radius of head nor radius of impactor, it can be emphasized that in the prediction of the HIC, the ellipsoidal model is the same as the spherical model.

In the present study, impacting at the head points of semi-axes  $a$ ,  $b$ , and  $c$  with varying mass and velocity of impactor were investigated to show the peak force transmitted and the impact duration. Compared with the spherical model at semi-axes  $a$  and  $b$ , the results appear to have higher values for the peak force transmitted and lower values for the impact duration, but at the semi-axis  $c$ , lower values for the peak force transmitted and higher values for the impact duration.

The analytical model presented can provide more accurate results in comparison with the existing analytical models. Furthermore, it can be used for investigating the effects of site of impact and the effect of inconstant shell thickness.

## References

- [1] THURMAN D., ALVERSON C., DUNN K., GUERRERO J., SNIEZEK J., *Traumatic brain injury in the United States: a public health perspective*, Journal of Head Trauma and Rehabilitation, 1999, 14(6), 602–615.
- [2] THURMAN D., *The epidemiology and economics of head trauma*, [in:] L. Miller, R. Ayes (eds.), *Head Trauma: Basic, Preclinical, and Clinical Directions*, John Wiley and Sons, New York, 2001, 327–347.
- [3] ANZELIUS A., *The effect of an impact on a spherical liquid mass*, Acta Pathologica et Microbiologica Scandinavica, Supplement, 1943, 48, 153–159.
- [4] GUTTINGER W., *Der Stosseffekt auf eine Flüssigkeitskugel als Grundlage einer physikalischen Theorie der Entstehung von Gehirnverletzungen*, Zeitschrift fuer Naturforschung, Teil A, 1950, 5, 622–628.
- [5] GOLDSMITH W., *The physical processes producing head injury*, [in:] Proceedings of the head injury conference, J. B. Lippincott Co., 1966, 350–382.
- [6] ENGIN A.E., *The axi-symmetric response of a fluid-filled spherical shell to a local radial impulse – a model for head injury*, Journal of Biomechanics, 1969, 2, 325–341.
- [7] KENNER V.H., GOLDSMITH W., *Dynamic loading of a fluid filled spherical shell*, International Journal of Mechanical Science, 1972, 14, 557–568.
- [8] YOUNG P.G., *An analytical model to predict the response of fluid-filled shells to impact – a model for blunt head impacts*, Journal of Sound and Vibration, 2003, 267, 1107–1126.
- [9] KHALIL T.B., VIANO D.C., *Critical issues in finite element modelling of head impact*, Proceedings of the 1982 Stapp Car Crash Conference, Michigan, USA, 1982, SAE paper # 821150, 87–102.
- [10] SAUREN A.A.H.J., CLAESSENS M.H.A., *Finite element modelling of head impact: the second decade*, Proceedings of the 1993 International IRCOBI Conference on the Biomechanics of Impact, Eindhoven, the Netherlands, 1993, 1–14.

- [11] VOO L., KUMARESAN S., PINTAR F.A., YOGANANDAN N., SANCES Jr. A., *Finite-element models of the human head*, Medical and Biological Engineering & Computing, 1996, 34, 375–381.
- [12] RAUL J.S., DECK C., WILLINGER R., LUDS B., *Finite-element models of the human head and their applications in forensic practice*, International Journal of Legal Medicine, 2008, 122, 359–366.
- [13] EL SAYED T., MOTA A., FRATERALI F., ORTIZ M., *Biomechanics of traumatic brain injury*, Computer Methods in Applied Mechanics and Engineering, 2008, 197, 4692–4701.
- [14] HERTZ H., *Ueber die Beruehrung fester elastischer Koerper*, Zeitschrift fuer die Reine und Angewandte Mathematik, 1882, 92, 156–171.
- [15] GOLDSMITH W., *Impact, the Theory and Physical Behavior of Colliding Solids*, Edwards Arnold, London, 1960, Table 6, p. 88.
- [16] GRAY A., *Modern Differential Geometry of Curves and Surfaces with Mathematica*, 2nd ed., Boca Raton, FL: CRC Press, 1997.
- [17] REISSNER E., *Stresses and small displacements of shallow spherical shells*, II, Journal of Mathematics and Physics, 1947, 25, 279–300.
- [18] YOUNG P.G., MORFEY C.L., *Intra-cranial pressure transients caused by head impacts*, Proceedings of the 1998 International IRCOBI Conference on the Biomechanics of Impact, Gothenburg, Sweden, 1998, 391–403.
- [19] JOHNSON E.A.C., YOUNG P.G., *On the use of a patient specific rapid prototyped model to simulate the response of the human head to impact and comparison with analytical and finite element models*, Journal of Biomechanics, 2005, 38, 39–45.
- [20] POSTON A., *Static adult human physical characteristics of the adult head*, Human Engineering Design Data Digest, Department of Defense Human Factors Engineering Technical Advisory Group (DOD HFE TAG), 2000, 72–75.